

ACOUSTIC-DOPPLER VELOCIMETER (ADV) FOR LABORATORY USE

Atle Lohrmann¹, Ramon Cabrera², and Nicholas C. Kraus³, M. ASCE

Abstract

A remote-sensing, three-dimensional (3D) velocity sensor has been developed and tested for use in physical model facilities. The sensor is based on the Acoustic Doppler principle and measures the 3D velocity at a rate of 25 Hz in a sampling volume of less than 1 cm³. The sensor is mechanically rugged, can be used in open-air physical model facilities, and can be readily moved from location to location with minimum setup time. A convenient interface operated on a PC allows instrument setup, file naming, and visual monitoring of the three flow components from simple menus. The instrument can replace several types of flow measurement instruments such as propeller gauges, electromagnetic gauges, Pitot tubes, LDVs, and hot-film anemometers, thereby simplifying procedures for technicians while providing continuous digital records at user-specified sampling rates.

Introduction

The development of the Acoustic-Doppler Velocimeter (ADV) was initiated under contract by the U.S. Army Engineer Waterways Experiment Station (WES) in 1992 to satisfy the need for an accurate current meter that can measure 3D dynamic flow in physical models. Such facilities include uniform-flow flumes, spillway models, 2D and 3D shallow-water wave basins, and outdoor near-prototype-scale riprap facilities. A requirements analysis conducted by two

¹ Senior Oceanographer, SonTek, 7940 Silverton Ave., #105, San Diego, CA 92126.
Tel (619) 695-8327, Fax: (619) 695-8131.

² Senior Engineer, SonTek.

³ Director, Conrad Blucher Institute for Surveying and Science, Texas A&M University -
Corpus Christi, TX 78412, Tel: (512) 994-2646, Fax: (512) 994-2715

laboratories at WES resulted in a development project to identify and implement a technology that would allow sub-centimeter resolution and minimum 25 Hz sampling rate while achieving a commercial unit cost of less than \$10,000. In addition, primary importance was attached to achieving measurements close to solid boundaries, easy integration with existing data-acquisition systems, and minimum need for recalibration.

To meet the requirements, a "bistatic" (focal-point) ADV was designed and built. The Doppler measurement technique, in contrast to the acoustic travel-time and electromagnetic techniques, has the advantage of being inherently drift-free and does not require routine recalibration. Also, acoustic pulses do not suffer the range limitations of optical (light) pulses in turbid water.

In the following sections, we describe the measurement principle and the instrument calibration, and then examine the size and shape of the sampling volume in some detail. We also report preliminary results from specialized applications such as ultra-low flows (<1 cm/s), characterization of turbulent parameters, and the possibility of using ADVs to make concurrent measurements of velocity and sediment concentration.

Principle of operation

Fig. 1 shows an overview of the ADV as implemented by SonTek (ADV-1). The system has three main modules: measurement probe, signal conditioning module, and signal processing module. In the present implementation [Kraus et al. 1994], three 10-MHz receive elements are positioned in 120° increments on a circle around a 10-MHz transmitter. The probe is submerged in the flow and the receivers are slanted at 30° from the axis of the transmit transducer and focus on a common sampling volume. The volume is located either 5 or 10 cm from the probe to reduce flow interference.

The transducer array is mounted at the end of a thin stem to

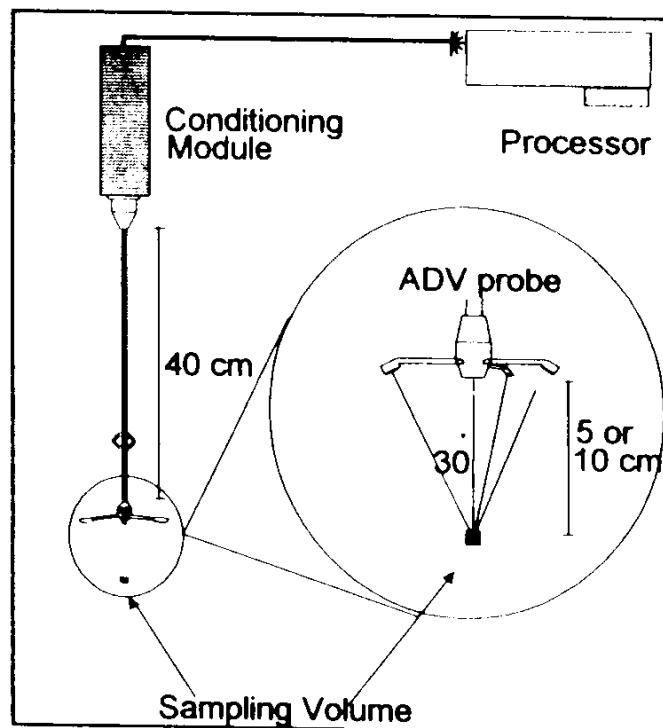


Fig. 1 The ADV-1 consists of a probe, a signal conditioning module, and a processing module.

facilitate installation of the instrument in typical laboratory setups, and to minimize flow interference by keeping the main bulk of the instrument away from the measured flow. The other end of the stem is attached to a 50-mm diameter, 300-mm long waterproof housing containing the signal conditioning module. This module contains all of the sensitive analog electronics that permit detection of the weak backscattered signals.

Digital signal processing and system control is performed by a single circuit card that fits into a 16-bit IO-slot of an IBM AT-compatible computer. This card contains a powerful signal processor that can perform the required computations for real-time estimation of 3-axis velocities at output rates up to 25 Hz. Electrical power for the signal conditioning module and for driving the transmit transducers is derived from the AT power bus so that no external power supply or other external components are needed.

Fig. 2 shows the basic measurement technique employed by an ADV. The system operates by transmitting short acoustic pulses along the transmit beam. As the pulses propagate through the water, a fraction of the acoustic energy is scattered

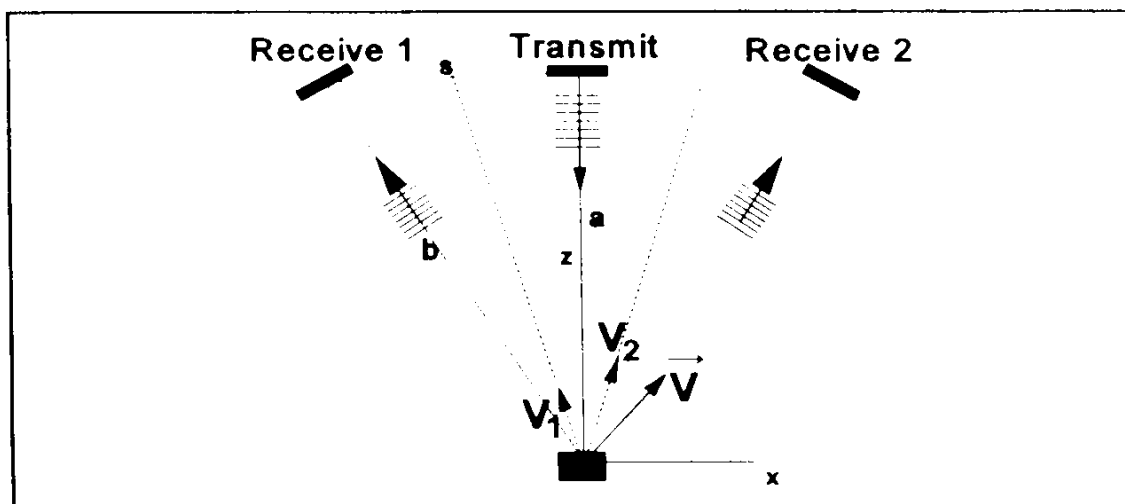


Fig. 2 Doppler Measurement Technique

back by small particles suspended in the water (e.g., suspended sediments, small organisms, etc.). The three receivers detect the "echoes" originating at the sampling volume, which are Doppler shifted due to the relative velocity of the flow with respect to the probe. The Doppler shift observed at each receiver is proportional to the component of the flow velocity (V_1 and V_2) along the bisector of the receive and transmit beams. Doppler shifts measured at the three receivers thus provide estimates of flow velocity along three different directions, which are then combined geometrically to obtain the three orthogonal components of the water velocity vector V .

The ADV-1 measures the three orthogonal components of the velocity vector within

a common sampling volume defined by the interception of the transmit and receive beams. The system uses pulse-to-pulse coherent Doppler techniques ([Miller and Rochwarger 1972], [Zrníc 1977], and [Lhermitte and Serafin 1984]) to achieve short term velocity errors of 1-10 mm/s at rates up to 25 Hz, even in highly variable flow conditions with peak velocities as high as 2.5 m/s. The processing algorithms are self-adaptive to avoid pulse-to-pulse interference when operating close to the surface or to a solid boundary.

Calibration

The calibration of the ADV is done in two steps. First, the exact probe geometry is determined. Although designed to a specification of 30°, the three angles between the transmit transducer, sampling volume, and receive transducers will vary slightly from probe to probe. The small variations in angle must be included in the calibration, and each probe has its own unique calibration table. The data are generated during factory testing and can be expressed as a transformation matrix T between the measured velocity V_1 with components V_1 , V_2 , and V_3 and the earth-referenced velocity vector V with orthogonal components V_x , V_y , and V_z :

$$V = \begin{bmatrix} \sin\phi_1\cos\theta & \sin\phi_1\sin\theta & \cos\phi_1 \\ \sin\phi_2\cos(\theta+2\pi/3) & \sin\phi_2\sin(\theta+2\pi/3) & \cos\phi_2 \\ \sin\phi_3\cos(\theta+4\pi/3) & \sin\phi_3\sin(\theta+4\pi/3) & \cos\phi_3 \end{bmatrix} * V_i \quad (1)$$

where ϕ_i represent the three calibration angles, and θ is the rotation around the z-axis (heading). Rotation around the x- and y-axis (pitch and roll) has been disregarded. The system is calibrated by running the probe three times in a tow tank; each time with a different heading. Detailed analysis of the full set of equations shows this technique to provide estimates of the calibration angles that are accurate to within 0.1°. The method does not require a high-precision mounting fixture and is robust with respect to small pitch and roll angles (<5°).

The geometry of the probe does not change unless it is physically damaged. Normally, any deformation can be detected by simple inspection but it is also possible to detect changes by using software utilities. If, for example, a receiver arm is twisted or bent, the receiver elements are no longer focused on the sampling volume. Consequently, the signal strength from the deformed receiver will display significantly reduced signal strength compared to the undamaged receiver arms. Because the signal strength is both displayed during data collection and recorded to file, probes that are bent will be detected. For deformations that are too small to be detected by a reduction in signal strength, there may be a small effect on the calibration. The geometry of the probe arms and the implementation of the signal

processing, however, prevent significant impact on the calibration. With reference to Fig.2, the total distance from the transmit to the receive transducer (s) is unlikely to change even if the probe arm is bent. Also, the total travel time for the signal ($a+b$) will not change since the sampling time is determined by the hardware. Any error in the calibration angle is thus subject to the following constraints:

$$\begin{aligned} s &= \text{constant} (= 25\text{mm}) \\ a+b &= \text{constant} (= 108\text{mm}) \end{aligned} \quad (2)$$

When solving the resulting systems of equations, it becomes apparent that small deformations in the receiver arm only result in very small errors in the horizontal velocity. For example, the calibration error is less than 1% even if the change in angle as a result of the deformation is as large as 5%.

The second part of the calibration is contained in the normal data collection procedure. Before each run, the speed of sound is calculated based on site-specific temperature and salinity values. The speed of sound can vary from 1440 m/s in cold, fresh water to 1540 m/s in warm, salt water. Without calibration, a nominal speed of sound of 1490 m/s could lead to errors as large as 3.3%. With routine calibration prior to each use, the error due to the speed of sound is limited to about 0.2% if the operator knows the temperature to within 1°C.

Sampling volume

The size of the sampling volume is determined by the length of the transmit pulse, the width of the receive window, and by the beam pattern of the transmit and receive beams. The first set of parameters defines the vertical extent of the sampling volume whereas the second set determines the width or horizontal extent. The latter can be approximated by the size of the transmit ceramic because a 7-mm ceramic vibrating at 10 MHz operates in the acoustic near-field out to 100 mm. In the near-field, the beam pattern is approximately cylindrical and the standard, 3-dB beam width is approximately equal to the size of the ceramic. In reality, this picture is simplified and the correct horizontal shape can only be derived by numerically integrating the joint nearfield beam patterns. The results show the horizontal weight function to be slightly asymmetric toward the receive transducer. The horizontal extent is thus slightly different for each of the three beams. From numerous velocity measurements, however, we have not been able to detect any results that would indicate that these differences are significant.

The vertical extent of the sampling volume is usually more important than the horizontal extent because of the precise positioning required in boundary layer experiments. For acoustic backscattering systems, the sampling volume is defined as the convolution between the transmit pulse and the receive window. In a typical configuration of the ADV, the transmit pulse is shorter than the receive window and the resulting weight function is flat, has a baseline of 9 mm, and the midpoint of the

sampling volume can be positioned as close as 4.5 mm from a solid boundary.

To get closer to a boundary, we can reduce the length of the transmit pulse or reduce the size of the receive window. The first is done at the penalty of a reduction in signal strength. The effect of this reduction is the same as the penalty for a decreasing the receive window: an increase in the Doppler noise. To estimate the mean current profile, however, we can reduce the Doppler noise by averaging over time. Both strategies are thus available and the smallest sampling volume has a vertical extent of about 0.6 mm. This means that the ADV, at least theoretically, can make measurement where the midpoint of the sampling volume is less than 1 mm from a solid boundary. In the case of a movable bed, the distance should be increased by 1 or 2 mm to allow for lateral variation in the bed profile and to permit bed movement within the averaging period.

Test results

Since the construction of the first prototype in January of 1993, several ADVs have been subjected to an extensive series of tests to verify their performance in a wide variety of operational conditions. Besides accuracy and temporal resolution, these tests addressed specialized topics such as flows less than 1 cm/s, response to the probe moving in and out of the water (such as might occur during wave motion), measurement of turbulent kinetic energy and Reynolds stress, response to high sediment concentrations, and directional response. The results from selected tests are briefly discussed here.

The first evaluation of the system was performed at WES [Kraus et al. 1994], where tests were conducted in a spillway model, a 2D wave basin, a 3D wave basin, a ship navigation model, and a near-prototype rip-rap circular channel. In these tests the measurements collected with the ADV were compared to those gathered with other velocity sensors routinely used at WES such as Laser Doppler Velocimeters (LDV), acoustic travel time sensors, pitot tubes, and surface height gauges. The ADV was successful in all tests, providing data that agreed well with those gathered by other velocity sensors. These tests also demonstrated the versatility and simplicity of use of the system. The ADV was easily installed, typically within a few minutes, in a variety of physical models, from small wave flumes to stream-size outdoor channels. It was also capable of operating in a wide range of flow regimes that included the breaker zone in a 3D wave basin and a hydraulic jump in a spillway model. Most comparisons had to be made based on the statistical characteristics of the velocity data such as the mean, standard deviation, and power spectra. This was due to the short spatial and time scales of the flow in the models, which resulted in slight disagreement in the instantaneous velocity measured by sensors placed at different locations. Other factors contributing to discrepancies in the instantaneous velocity were differences in the sampling volume and response time.

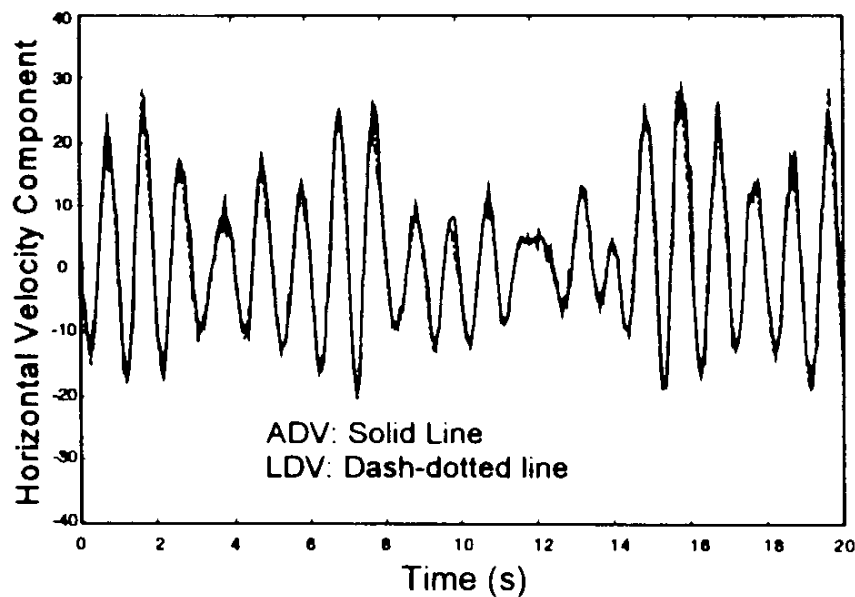


Fig. 3 - Horizontal velocity from ADV and LDV in wave flume.

Fortunately, the 2D wave basin provided an opportunity for a direct comparison of instantaneous velocities. In this test, the sampling volumes of the ADV and that of a 2D Dantec LDV were aligned visually so that both instruments would measure flow velocities from approximately the same volume of water. The still-water depth in the wave channel was 0.3 m, and the sampling volume of both instruments was located approximately 0.15 m below the mean water surface. The LDV was set to sample at 50 Hz and the ADV at 25 Hz. Fig. 4 compares measurements of the horizontal component of wave orbital velocity measured with the ADV (solid line) and the LDV (dash-dotted line). The broadband waves had a mean period of 1.0 s and an RMS wave height of 0.15 m. The plot shows good visual agreement in shape and peak of the oscillatory signals from the two instruments. Linear regression was performed on the data sets, generating a slope of 1.03 and an offset of 0.11 cm/s. Good agreement was also obtained for the weaker vertical velocity component.

Tow-tank tests

Tow-tank tests of the ADV were conducted at NorthWest Research Associates, Inc (NWRA) in Bellevue, Washington. The NWRA channel is 9.75 m long, 0.91 m wide, and 0.91 m deep. The ADV probe was attached to a tow carriage mounted on top of the channel and driven by an electrical motor. The speed of the carriage is determined independently by a tachometer, and by the time required for a 25.4-cm long bar, mounted horizontally on the carriage, to pass three sets of optical sensors located on the channel wall (giving three additional speed measurements). The standard deviation of these four speed estimates was calculated to be 0.2% over the range 1 to 250 cm/s.

The purpose of these tests was to verify the linearity of the ADV velocity measurements over its full dynamic range, ± 2.5 m/s. As with any instrument, the

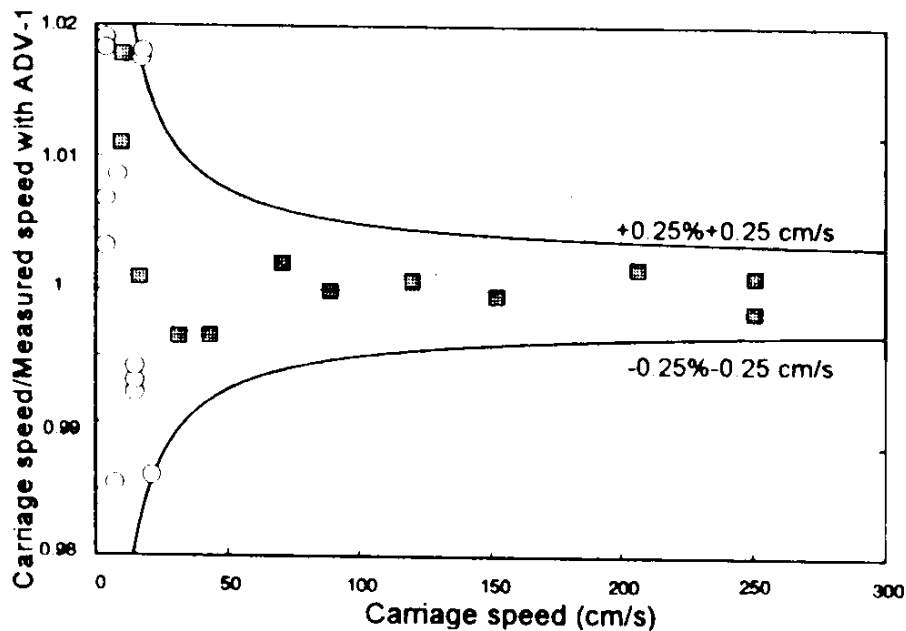


Fig. 4 - ADV Linearity over full range. Data collected at NWRA (squares) and at USGS/Stennis Space Center (circles).

importance of linearity lies in the calibration. As describe previously, the velocity vector is computed from the three measured along-beam velocities by using a transformation matrix that incorporates the relative position and orientation of the four acoustic transducers. If the system is linear, the transformation matrix can be determined empirically by calibrating the system at one speed, and will remain constant as long as the physical dimensions and geometry of the probe remain unchanged.

Fig. 4 shows the ratio between carriage speed and along-channel velocity component over carriage speeds from 10 to 250 cm/s. The output is linear to better than 0.25% over a range of 15 to 250 cm/s. Strong linearity assures a highly accurate 3D velocity measurement system over the full velocity range and makes it possible to calibrate the instrument in a single-speed tow channel.

Below 15 cm/s, the test at NWRA showed a small bias of the ADV toward lower velocities. The bias was caused by a hardware problem that was subsequently corrected. Later low-speed tests at the tow tank operated by the U.S. Geological Survey at the Stennis Space Center showed (Fig. 4 - circles) that the bias was no longer present and that the ADV can be accurate to within $\pm 0.25\% \pm 0.25$ cm/s over its full velocity range if properly calibrated.

Performance at low flows

An example of the ADV capability for measuring low-velocity flows is given by the time series of velocities shown in Fig 5. This data set was collected with the ADV measurement probe immersed in a 1-gallon bucket of water, collecting data at a rate of 25 Hz. The oscillations were initiated by tilting the bucket slightly then letting it

rest. The plot shows how well the ADV can resolve a 2-Hz sinusoidal signal with an amplitude of less than 1 cm/s.

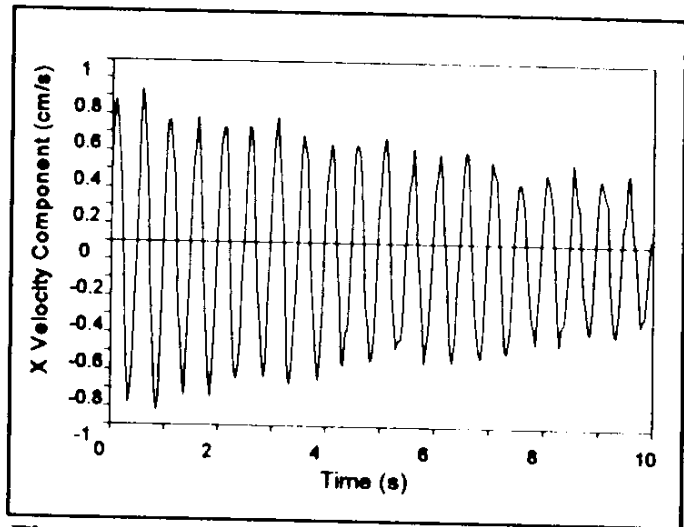


Fig. 5 - Time series of one horizontal velocity component collected with an ADV in a small bucket of water.

A special mode of operation has recently been developed that allows the ADV to measure very low flows with accuracies better than 0.1 mm/s over velocity ranges of up to a few cm/s. This mode of operation was tested at the borehole calibration facility at the U.S. Geological Survey in Denver. During the tests, the probe was submerged in a cylinder of diameter 0.1 m. The flow is controlled with a pump and the setup is designed to simulate the conditions in a well or in a borehole. The simulation is complicated by thermally driven circulation that persists until the air and water temperature have stabilized. The convective currents are of the same order as the net transport rate, and we subtracted 1.8 mm/s from the measured vertical velocity to account for the circulation at the position of the probe. After this correction, the 3-minute mean vertical velocity was plotted on a loglog scale (Fig. 6). The

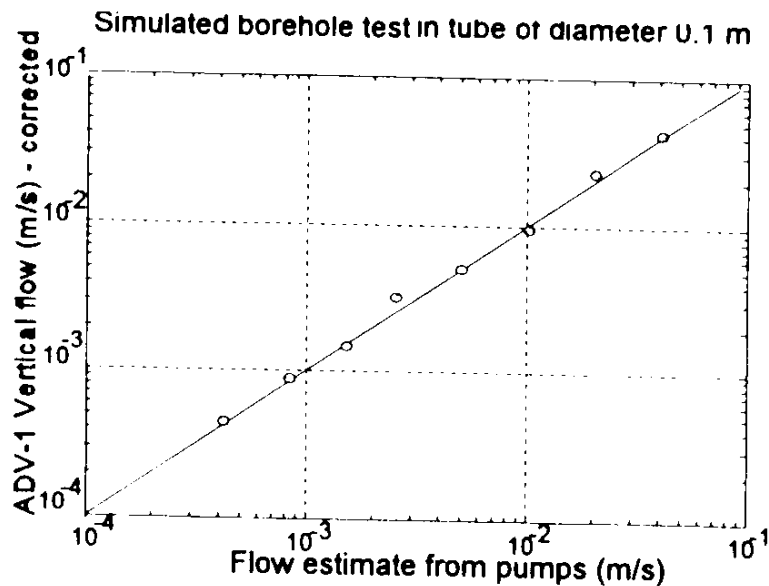


Fig. 6 - Calibration at low flows. The solid line is the 1:1 curve and the circles depict the data points.

agreement between the calibrated pumps and the ADV is quite good all the way down to the minimum test velocity of 0.4 mm/s. Toward the end of the day, when the pumps were turned off and the water was in approximate thermal equilibrium, the measured vertical velocity was 0.04 mm/s and the mean horizontal velocity

0.015 mm/s (= 0.003 ft/min = 4.5 ft/day). This gives credence to the hypothesis of a 1.8 mm/s thermally driven circulation. Also, these minimum velocities are close to what we previously have seen in laboratory experiments and they probably represent a good estimate of the sensitivity of the ADV.

Turbulence measurements

The relatively high temporal resolution and small sampling volume of the ADV implies that it is possible to measure field and prototype scale turbulence on a routine basis. Practical tests have also shown that the resolution is sufficient to capture a significant fraction of the turbulent kinetic energy and Reynolds stress within the bottom boundary layer of most laboratory flumes.

The short-term error, or the Doppler noise, is an inherent part of all Doppler-based backscatter systems. It represents a fundamental aspect of the measurement process and is related to the random distribution of the particles that contribute to the acoustic echo. The magnitude of Doppler noise is a function of the signal strength but also depends strongly on the flow condition itself. Unfortunately, it is not always easy to predict its magnitude in advance of an experiment because there always is a degree of uncertainty with respect to the exact flow conditions.

There are three aspects of the Doppler noise that should be noted: a) the noise can be reduced by averaging over independent realizations, b) the noise from two independent channels is uncorrelated, and c), the noise is white in the spectral domain. The possibility of reducing the noise by averaging is important because it means that the magnitude and the importance of Doppler noise will diminish as the averaging period increases.

For the purpose of describing the effect of Doppler noise on turbulence measurements, we separate the measured velocity components V_i into a "mean" velocity and a fluctuating part that contains turbulent energy V_i' and Doppler noise V_{di} :

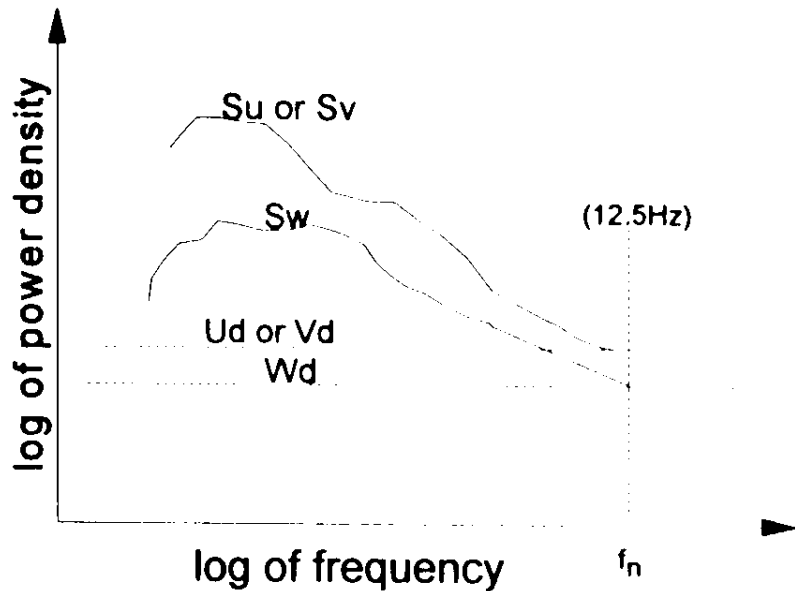
$$V_i = \bar{V}_i + V_i' + V_{di}, \quad \overline{V_i' + V_{di}} = 0, \quad \overline{(V_i' + V_{di})^2} = \overline{V_i'^2} + \overline{V_{di}^2} \quad (3)$$

The first two expressions are definitions, whereas the third expression incorporates the fact that the time-averaged product between natural fluctuations and the Doppler error is zero. This is an important aspect of the noise and allows the calculation of quantities that are smaller than the Doppler noise.

The relationship between the beam velocities with subscript i and the orthogonal velocity components can be described by the matrix $A = \text{inv}(T)$ with elements a_{ij} . The turbulent kinetic energy can then be expressed as:

$$|V^2| = \sum ((AV'_i)^2 + (AV'_{di})^2) \tag{4}$$

The Doppler noise enters directly into the equation and the measured energy will be biased high. The bias scales with $(V_{di}/V'_i)^2$ and will be small in high-energy situations such as boundary layer flow. In oscillatory flow, the turbulence level can be estimated in the same way as the dissipation rate by analyzing the energy level of the saturation range in the velocity spectrum.



Because the Doppler noise is white it is easily identified as a "noise floor" (See fig. 7) and its signature is a flattening of the spectrum (S_u , S_v , or S_w) as we approach the Nyquist frequency (f_N) at 12.5 Hz in the case of a standard ADV-1.

Fig. 7 - Typical power spectrum for the ADV. The Doppler noise is higher for the horizontal components (U_d , V_d) than for the vertical component (W_d).

In the worst case this may take place around 4-5 Hz for the horizontal velocity but more typically in the range 5-10 Hz. For the vertical velocity, the noise floor rarely plays any role below the Nyquist frequency, and this is the component of choice in case of isotropic turbulence. For fully developed turbulence with a well-defined spectral equilibrium range we can extract the turbulent kinetic energy (or the dissipation rate) by transforming the frequency spectrum to a wave number spectrum and then using the appropriate scaling.

The Reynolds stresses are typically smaller than the turbulent kinetic energy and often smaller than the Doppler noise. If the receive beams were orthogonal, i.e. $V_i = V$, this would not be a problem because the Doppler noise in two independent channels is uncorrelated and the estimate of the Reynolds stress would be independent of the magnitude of the Doppler noise. In the case of an ADV, however, the receive beams are not orthogonal and Reynolds stress must be derived using the matrix **A**. If we let the x, y, and z-coordinates be defined by the probe geometry, we can write:

$$\begin{aligned} \overline{u'w'} = & a_{11}a_{31}(\overline{V_1'^2} + \overline{V_{d1}^2}) + a_{12}a_{32}(\overline{V_2'^2} + \overline{V_{d2}^2}) + a_{13}a_{33}(\overline{V_3'^2} + \overline{V_{d3}^2}) + \\ & (a_{11}a_{32} + a_{31}a_{12})\overline{V_1'V_2'} + (a_{11}a_{33} + a_{31}a_{13})\overline{V_1'V_3'} + (a_{12}a_{33} + a_{32}a_{13})\overline{V_2'V_3'} \end{aligned} \tag{5}$$

The first line contains three terms that all involve the total variance of the along-beam velocity. The second line only contains terms with cross-products between beams and the uncorrelated Doppler noise has no contribution. If we sum up the constants in the first line ($a_{11}a_{32} + a_{12}...$) we find that the sum is zero, and it would be simple to conclude that the contribution from the first line is zero. In an experiment conducted by the U.S. Geological Survey, St. Petersburg, in a flume located at the University of South Florida, this proved not to be true. Instead, the contribution was evenly split between the first and the second line, implying that the asymmetry in the along-beam variance is important. The contribution of the Doppler noise, however, is zero as long as the Doppler noise is the same in all beams. Because the Doppler noise is a function of the signal strength this means that the signal strength should be the same in all three beams. This turned out not to be the case of the ADV used in the St. Petersburg experiment, where a constant, positive offset can be observed at low flows in Fig 8. At higher flows, the slight asymmetry in the Doppler noise becomes negligible and the match between the data collected with a Dantec LDV and the ADV is quite good.

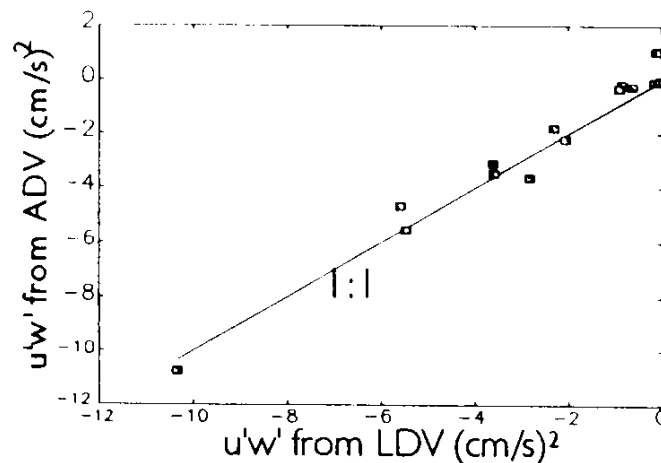


Fig. 8 - Turbulent stress measurements from flume. The straight line depicts a 1:1 relationship between the LDV and the ADV.

In sum, an ADV can be used to measure turbulent kinetic energy in excess of the Doppler noise and/or indirectly estimate the energy as long as the saturation range in the spectrum can be resolved. The sensitivity to Reynolds stress is not limited by the magnitude of the Doppler noise but by how well the Doppler noise is balanced in the three receive channels.

Scattering measurements

There are two aspects of scattering measurements that are of interest here. The first affects the velocity measurements directly through the functional relationship between the signal strength and Doppler noise. If the signal strength is too weak, as may be the case in quiescent basins or in stationary flumes, the Doppler noise becomes high and the introduction of small particles (seeding) may be required. To

ensure that this information is available both during the data collection and during postprocessing, the software displays and stores the signal-to-noise ratio (SNR) of the scattered signal. The noise level N is measured at the beginning of each measurement sequence and is close to the electronic noise level for the ADV. The signal strength I is measured each time the receivers are turned on to measure the velocity and the signal-to-noise ratio is defined as:

$$SNR = 10 \log_{10} \left[\frac{I}{N} \right] \quad (6)$$

As mentioned previously, the Doppler noise varies with the SNR. In our experience, an SNR of 15 dB is sufficient to obtain reasonably low-noise data at 25 Hz, whereas a ratio of about 5 dB is sufficient to obtain good quality data at 1 Hz.

The second reason for measuring the scattered intensity I is the potential for extracting information about the concentration of particles in the sampling volume [Hay, 1991]. Although the details can be algebraically complex, a simplified version of the problem can be expressed as:

$$I = I_0 C S_p S_r \frac{e^{-2(\alpha_w + \alpha_p) r}}{r^2} \quad (7)$$

where I_0 is the transmitted intensity, C is the particle concentration, α_w is the water absorption, α_p is the attenuation due to particle scattering, r is the acoustic propagation path, S_p holds all the particle specific parameters (size, elasticity, and density), and S_r contains all the system specific parameters such as transducer size, efficiency, probe geometry, receive sensitivity, as well as the full nearfield expression for the pairs of transmit and receive beams.

From the equation, it can be seen that the scattering strength increases in proportion to the concentration. Unfortunately, the echo is also modified by increased particle attenuation, and a plot of concentration versus intensity [Schaafsma and der Kindem, 1985] will show a near-linear relationship for low and intermediate concentrations (< 1 g/l) and then exhibit strong non-linear features before the attenuation finally becomes strong enough to reduce the intensity I below an acceptable level of SNR. The span of concentrations over which it is possible to measure velocity is thus much larger than the span over which the measured intensity is proportional to concentration.

It should be added that the above equation is only valid if the particle size distribution remains constant. If $ka < 1$, where k is the acoustic wave number and a is the particle radius, the scattering is proportional to the square of the particle volume and thereby sensitive to the exact size distribution. For $ka > 1$ ($a > 24 \mu\text{m}$ in case of a 10 Mhz system) the scattering is proportional to the surface area. This

size-dependency is the same as that of an optical backscatter sensor (OBS) and the scattering characteristics for the two instruments are similar for "large" particles.

Conclusions

The ADV has proven to be a versatile and accurate 3-D velocity sensor suitable for most applications in physical models. The overall assessment from previous studies [Kraus et al 1994] shows the ADV to have: (1) somewhat less temporal and spatial resolution but comparable accuracy to a laser-Doppler velocimeter (LDV); (2) added benefit of providing full three-axis velocity measurement; (3) good penetration in turbid water; (4) significant improvements in operational simplicity and versatility as compared to LDVs; (5) one-tenth the cost of a conventional LDV, and (6) ruggedness and convenience of measurement in difficult-to-reach areas in the flow compared to time-of-flight acoustic flow meters or LDVs. The accuracy of the system has been reaffirmed in additional tow tank tests, and the linearity has proven to be within $\pm 0.25\%$.

In addition, the ADV has been shown to be suitable for low-flow applications. Calibration at the borehole facility at U.S. Geological Survey in Denver suggests that reliable data can be obtained down to the minimum test velocity of 0.4 mm/s and possibly an order of magnitude lower. Estimates of turbulent kinetic energy are limited by the Doppler noise but alternative estimation techniques can be employed to take advantage of the fact that Doppler noise is white and eliminate bias in the energy or dissipation estimate. Comparison with an LDV shows that the Reynolds stresses can be accurately determined even at levels below the Doppler noise and that care must be taken to construct systems with a balanced SNR. Finally, the linearity between SNR and the logarithmic concentration of suspended sediments points to the possibility of measuring the velocity and concentration in a single volume. Although limited by size-sensitivity and particle attenuation at high concentrations, this methodology holds promise and will be further explored in upcoming experiments. These experiments will take advantage of the recent development of a PC-independent electronics module that allows integration with a self-contained data acquisition system and permits increased use in short-term field applications.

Acknowledgements

We sincerely appreciate the assistance of numerous WES staff members during the requirements analysis and tests of the ADV. We also appreciate the assistance of Dr. Yogesh Agrawal and Mr. Lee Piper at NWRA in the tow tank test. Dr. John Haines and Dr. Guy Gelfenbaum of USGS in St. Petersburg collected and analyzed the turbulence data.

References

- Hay, A., 1991: "Sound Scattering from a particle-laden, turbulent jet", *J. Acoust. Soc. Am*, Vol 90, No 4, 2055-2074.
- Kraus, N. C., Lohrmann, A., and Cabrera, R., 1994: "New Acoustic Meter for Measuring 3D Laboratory Flows", *J. Hydraulic Engineering*, Vol 120, No.3 , 406-412.
- Lhermitte, R. and Serafin, R., 1984: "Pulse-to-pulse coherent Doppler signal processing techniques", *J. Atmos. and Oceanic Technol.*, 1, 293-308.
- Miller, K.S. and Rochwarger, M.M., 1972: "A covariance approach to spectral moment estimation", *IEEE Trans. Inform. Theory*, IT-18, 588-596.
- Schaafsma, A.S. and der Kindern, W.J.G.J, 1985: "Ultrasonic instruments for the continuous measurement of suspended sand transport", *Symp. on Measuring Techniques in Hydraulic Res.*, Delft, 22-24 April, 1985
- Zrnica, D.S., 1977: "Spectral moment estimates from correlated pulse pairs", *IEEE Trans. Aerosp. and Electron. Syst.*, AES-13, 344-354.